Heparin binding to platelet factor-4

An NMR and site-directed mutagenesis study: arginine residues are crucial for binding

Kevin H. MAYO,*‡ Elena ILYINA,* Vikram ROONGTA,* Moira DUNDAS,† Jacqueline JOSEPH,† C. K. LAI,† Ted MAIONE† and Thomas J. DALY†

*Department of Biochemistry, Biomedical Engineering Center, University of Minnesota, 420 Delaware Street, Minneapolis, MN 55455, U.S.A. and †Repligen Corporation, 1 Kendall Square, Building 700, Cambridge, MA 02139, U.S.A.

Native platelet factor-4 (PF4) is an asymmetrically associated, homo-tetrameric protein (70 residues/subunit) known for binding polysulphated glycosaminoglycans like heparin. PF4 N-terminal chimeric mutant M2 (PF4-M2), on the other hand, forms symmetric tetramers [Mayo, Roongta, Ilyina, Milius, Barker, Quinlan, La Rosa and Daly (1995) Biochemistry **34**, 11399–11409] making NMR studies with this 32 kDa protein tractable. PF4-M2, moreover, binds heparin with a similar affinity to that of native PF4. NMR data presented here indicate that heparin (9000 Da cut-off) binding to PF4-M2, while not perturbing the overall structure of the protein, does perturb specific side-chain proton resonances which map to spatially related residues within a ring of positively charged side chains on the surface of tetrameric PF4-M2. Contrary to PF4–heparin binding models which centre around C-terminal α-helix lysines, this study indicates that a loop containing Arg-20, Arg-22, His-23 and Thr-25, as well as Lys-46 and Arg-49, are even more affected by heparin binding. Site-directed mutagenesis and heparin binding data support these NMR findings by indicating that arginines more than C-terminal lysines, are crucial to the heparin binding process.

INTRODUCTION

Human platelet factor 4 (PF4) (70-amino-acid residues/monomer) [1], which belongs to a family of CXC chemokines [2], demonstrates various physiological effects: it accelerates thrombin–anti-thrombin complex formation [3]; stimulates fibroblast attachment to the substrate [4]; stimulates histamine release from human basophils [5]; displays chemotactic activity with respect to neutrophils [6], monocytes [6,7], and fibroblasts [8]; potentiates platelet aggregation [9] and elastase release [10]; releases lysosomal enzymes from leucocytes [11]; reverses the immunosuppressive effect of lymphoma cells [12]; and inhibits megakaryocytopoiesis [13,14], angiogenesis [15], solid tumour growth [16] and vascular endothelial cell migration [17]. Many of these biological activities of PF4 appear to be related to its interaction with cell-surface glycosaminoglycans via a protein surface binding domain.

The best known PF4 activity is its ability to bind strongly to the anticoagulant heparin, a polysulphated glycosaminoglycan. When released by activated platelets during coagulation [18], PF4 displaces thrombin from heparan sulphate on the surface of endothelial cells [where thrombin is anticoagulant through its accelerated interactions with antithrombin III (AT-III), thrombomodulin and protein C] into solution, where thrombin is procoagulant through its interactions with fibrinogen and other clotting factors [3]. PF4 prevents the formation of the ternary complexes between heparin, AT-III, and various procoagulant serine proteases that are intermediate in the heparin-accelerated inhibition of proteases by AT-III.

In its native state, PF4 exists as a tetramer [19] in a complex with a high-molecular-mass proteoglycan carrier [20]. PF4 also binds with unusually high affinity to insolubilized heparin and binds to other less sulphated glycosaminoglycans with lower affinity [21]. Most of the heparin molecule (75–85 %) is accounted for by a repeating disaccharide unit that consists of L-ido-pyranosyluronic acid (IdoA) 2-sulphate and 2-deoxy-2-sulphamido-D-glucopyranose ($GlcNSO_3$) 6-sulphate [22–24]. The balance of the molecule is constituted largely of residues of 2-acetamido-2-deoxy-D-glucose and D-glucuronic acid, although the modes of bonding and distribution within the polymer, as well as their degrees of sulphation, have yet to be established unequivocally. In the presence of an excess of heparin (11 000 Da cut-off), the typical PF4–heparin complex consists of one 36-saccharide-long heparin molecule per protein tetramer [25], although two hexadecasaccharides also can bind to one PF4 molecule [26]. Since PF4 binds to glycosaminoglycans roughly in order of their negative charge density, that is, heparin ≥ heparan sulphate > dermatan sulphate > chondroitin sulphates > hyaluronic acid [27], the tetramer transfers easily to more sulphated polysaccharides such as heparin when the carrier complex is released from platelets.

X-ray crystallographic and NMR structural studies of bovine [28] and human [29,30] tetrameric PF4 show that all monomeric subunits have a three-stranded antiparallel β-sheet domain on to which is folded an amphipathic C-terminal α-helix and an aperiodic N-terminal domain. The amino acid sequence and general folding pattern of PF4 are shown schematically in Figure 1. In both human and bovine PF4 crystal structures, the homotetrameric arrangement of A, B, C and D subunits is asymmetric, with symmetric AB and CD dimers associating in a non-symmetric fashion. Substitution of the highly acidic N-terminal decapeptide segment of native human PF4 with the N-terminal sequence from homologous interleukin-8 (IL-8) (see Figure 1 for sequence comparison) results in formation of a symmetric PF4 tetramer (called PF4-M2) [30]. The strength of heparin binding to native PF4 and PF4-M2 is essentially

Abbreviations used: AT-III, antithrombin III; DTT, dithiothreitol; 2D-NMR, two-dimensional NMR spectroscopy; F-hep, fluorescein-derivatized heparin; FGF-2, fibroblast growth factor 2; IdoA, L-ido-pyranosyluronic acid; IL-8, interleukin-8; HOHAHA, homonuclear Hartmann–Hahn 2D-NMR spectroscopy; NOESY, 2D-NMR nuclear Overhauser effect spectroscopy; NOE, nuclear Overhauser effect; PF4, native platelet factor 4; PF4-M2, platelet factor-4 chimeric mutant containing the N-terminal 8 residues from interleukin-8.

‡ To whom correspondence should be addressed.

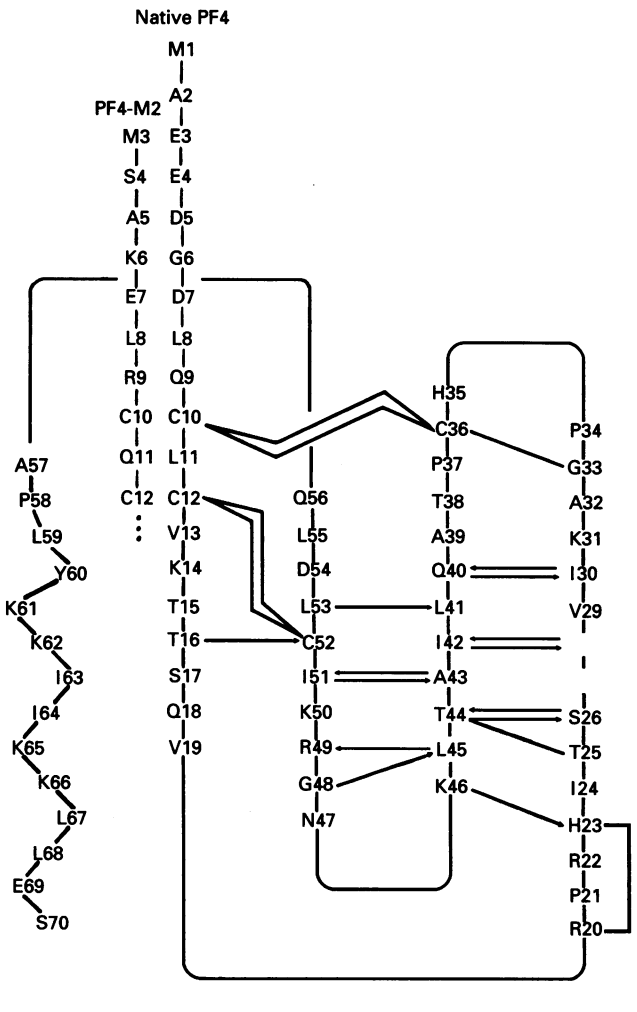

Figure 1 Sequence and schematic folding pattern for PF4 and PF4-M2

The complete amino acid sequence for native PF4 is shown. For PF4-M2, 11 N-terminal residues present in native PF4 have been replaced by eight N-terminal residues from homologous IL-8. PF4-M2 N-terminal residues are also shown. Residues 12–70 are identical for both species. In addition, the general folding pattern for both PF4 and PF4-M2 is indicated as described in the text. The two cystine disulphide bonds are shown as open bent bars, and some proposed hydrogen bonds are indicated by arrows.

the same [30], indicating that this asymmetry in native PF4 may be inconsequential to the heparin-binding process.

It has been proposed [1,25] that two pairs of lysine residues within the C-terminal α-helices of each monomer subunit are important for binding to heparin. Based on this information and assuming that native PF4 associates symmetrically, Cowan et al. [31] proposed a model for heparin binding to PF4, which has the anionic heparin polysaccharide wrapped about the tetramer and running parallel to the C-terminal α-helices. Using the X-ray structure of bovine PF4, which showed the presence of a ring of positive charge (which included the solvent-accessible C-terminal lysines) about the PF4 tetramer, Stuckey et al. [32] proposed an alternative PF4–heparin binding model using a graphically designed heparin molecule and the crystallographic coordinates of the native bovine PF4 tetramer. The Stuckey model of heparin bound to PF4 has the anionic polysaccharide running perpendicular to the α-helix axes wrapped about the tetramer along the ring of positive charge, and salt linked to all four lysines on the helix of each monomer.

In the present study, heparin binding to native PF4 and PF4-M2 is studied by using NMR spectroscopy and mutagenesis. Results generally support the perpendicular PF4–heparin binding model [32], but indicate that heparin interacts more effectively with the arginines in PF4 and less so with the C-terminal lysines.

MATERIALS AND METHODS

Isolation of recombinant PF4-M2 and native PF4

The synthetic genes for human PF4-M2 chimeric mutant and native PF4 were expressed as non-fusion proteins in *Escherichia coli* (BL21 DE3) cells and grown at the 2-litre (shake flask) or 10-litre (fermenter) scale. Protein was purified, cleaved and refolded essentially as previously described [33]. Cells were grown for 4 h followed by induction with isopropylthiogalactoside overnight, suspension in lysis buffer [0.05 M Tris/HCl, pH 8, 5 mM EDTA, 5 mM dithiothreitol (DTT), 0.1 % Triton X-100] and sonication in the presence of 0.1 % PMSF. The lysed preparation was treated with several aliquots of DNase 1, concomitantly added with $MgCl_2$ and incubated for 0.5 h at 4 °C. The suspension was then centrifuged at 13000 rev./min and the precipitate extracted in 0.05 M Tris/HCl, pH 8.0, 6 M guanidine hydrochloride, 50 mM DTT overnight at room temperature. The extracted material was dialysed against buffer containing 25 mM sodium acetate, pH 4.0, 8 M urea, 50 mM DTT and loaded on to an S-Sepharose column equilibrated with 25 mM sodium acetate, pH 4.0, 8 M urea. The urea was removed and the protein eluted in 50 mM Tris/HCl, pH 8.0, 1 M NaCl. Fractions containing protein were subjected to refolding overnight in the presence of 1 mM oxidized:2 mM reduced glutathione at room temperature. The extent of refolding was monitored by Poros analytical chromatography. The refolded species was rechromatographed using C_4 preparative or C_4 semi-preparative reverse-phase HPLC using a 0–100 % acetonitrile gradient in 0.1 % trifluoroacetic acid. Peak fractions were pooled and lyophilized for concentration determination and purity assessment. Purity was assessed by SDS/PAGE and analytical C_4 reverse-phase HPLC and amino acid analysis. Typically, several hundred milligrams of more than 95 % pure material was isolated from 100 g of starting material.

Nitrocellulose filter binding

Various concentrations of protein were incubated in the presence of $< 10^{-9}$ M [^{35}S]heparin (Cambridge Isotope, Inc., Cambridge, MA, U.S.A.) in buffer containing 10 mM Tris/HCl, pH 8.0, 150 mM NaCl, 50 μg/ml BSA (Binding buffer). The total volume for each assay tube was 0.5 ml. Samples were incubated for 1 h at room temperature. Samples were filtered through presoaked (in Binding buffer without BSA) 0.45 μm-pore-size nitrocellulose filters. Protein concentrations were tested in duplicate. Filters were dried and quantified by scintillation counting. Data were plotted as log (molar protein concentration) versus fractional saturation. Background levels were subtracted from all samples. The equilibrium dissociation constant was determined as the protein concentration at 50 % fractional saturation.

Solution-based fluorescein-derivatized heparin binding

Binding of native PF4 and PF4 mutants was examined by monitoring the quenching of heparin-based fluorescence. Fluorescein-derivatized heparin (F-hep) [34] was added to 3 ml of PBS. Excitation and emission were monitored at 488 nm and 520 nm respectively. Protein was titrated in small volume aliquots, with changes in fluorescence intensity being observed

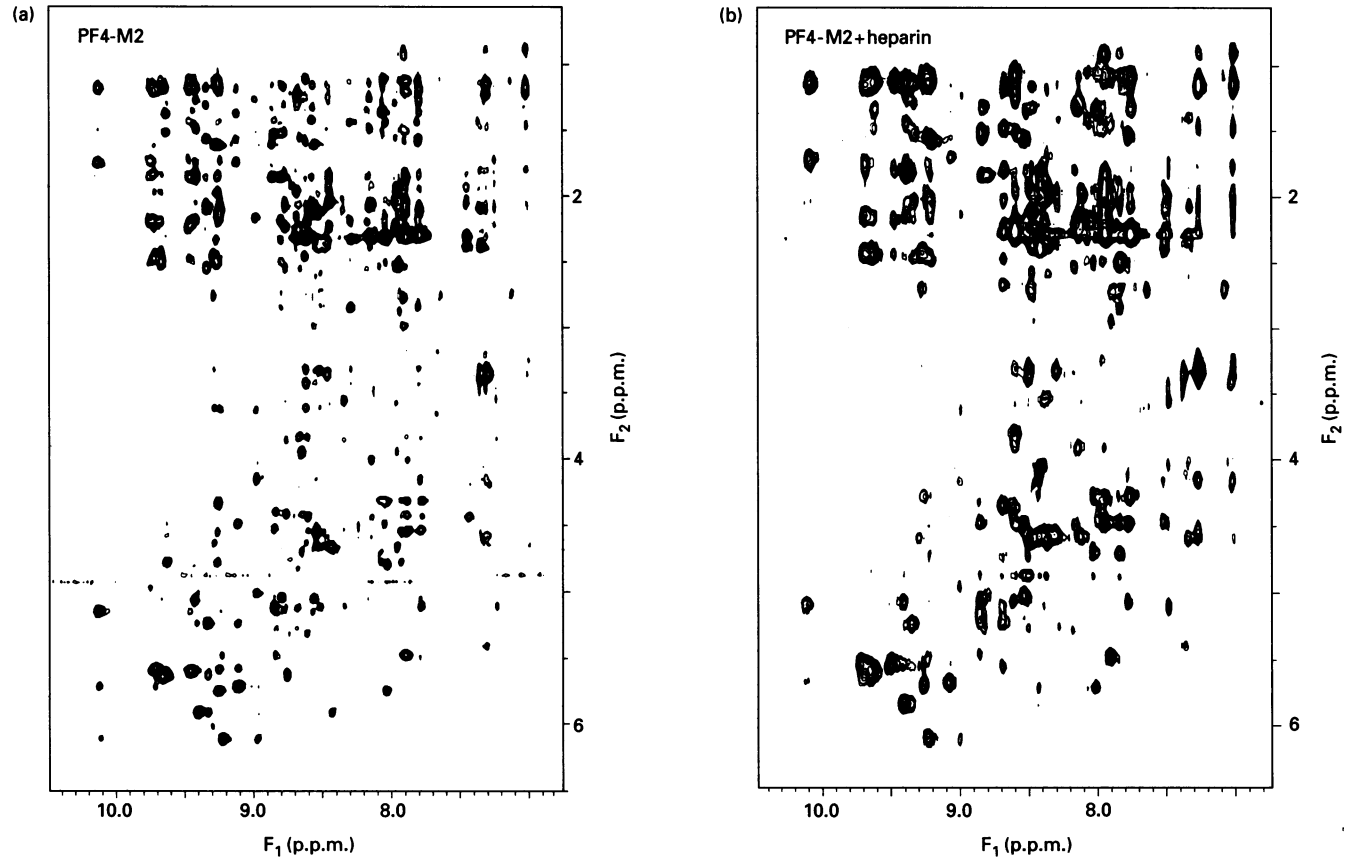

Figure 2 NOESY spectra of PF4-M2 with and without heparin

Two-dimensional-NMR NOESY contour plots are shown for PF4-M2 (2.3 mM in monomer), pH 5.9, 50 °C and 20 mM NaCl in 90% H_2O/10% ^2H_2O, in the absence (**a**) and presence (**b**) of heparin (9000 Da cut-off). The NOE mixing time in both spectra was 100 ms. Acquisition datasize was 1024 × 400 and processed datasize is 1024 × 1024. Water suppression was achieved by direct saturation of the water resonance for 0.8 s. Data were processed by multiplying the free induction decays by a shifted sine-bell function in both dimensions prior to Fourier transformation. Resonances and cross-peaks are labelled as described in the text.

between each protein addition. Titration curves were corrected for dilution and photobleaching effects by titration of F-hep with buffer controls. Following each protein addition, 5 min incubations were performed to reach the new equilibrium. Data were plotted as the concentration of protein versus the fraction of the maximal quenching of the corrected curves. Equilibrium binding constants were determined at the concentration of protein at 50% fluorescence quenching.

Determination of protein concentration

Protein concentrations were determined using the bicinchoninic acid (BCA) assay [35] and calculated on the basis of protein concentrations obtained from a standard dilution series of BSA. Amino acid analysis of these chemokines was obtained following hydrolysis of the proteins for 24 h at 90 °C in 12 M HCl. Samples then were derivatized and analysed according to the method of Bidlingmeyer et al. [36]. Protein concentrations also were checked by the methods of Lowry et al. [37] and of Waddell [38].

NMR spectroscopy

PF4-M2, which shows nearly the same heparin-binding activity as native PF4, was used for NMR studies. PF4-M2 forms symmetric tetramers making spectral analysis tractable [30]. Samples for NMR measurements had been lyophilized and redissolved in ^1H_2O or ^2H_2O immediately before the experiment. For work in ^1H_2O solutions, 10% ^2H_2O was routinely used. The final PF4-M2 concentration was 18 mg/ml. The pH was adjusted to pH 5.9 by adding microlitre increments of NaO^2H or ^2HCl to a 0.6 ml sample. The pH was not corrected for isotope effects.

NMR spectra were recorded in the Fourier mode on a Bruker AMX-600 spectrometer (600 MHz for protons). The ^2H_2O deuterium signal was used as a field-frequency lock. All chemical shifts are quoted in parts per million (p.p.m.) downfield from sodium 4,4-dimethyl-4-silapentane sulphonate (DSS).

For sequential assignments, COSY [39,40], double-quantum-filtered COSY [41,42] and two-dimensional nuclear Overhauser effect spectroscopy (NOESY) [40,44] experiments (mixing times of 0.05 s, 0.075 s, 0.1 s and 0.2 s) were performed. Two-dimensional (2D) homonuclear Hartmann–Hahn magnetization transfer (HOHAHA) spectra, used to identify many spin systems completely, were obtained by spin-locking with an MLEV-17 sequence [45] with mixing times of 30 to 60 ms. All spectra were acquired in the phase-sensitive mode by using time proportional phase incrementation (TPPI) or States-TPPI [46,47]. The water resonance was suppressed by direct irradiation (0.6 s) at the water frequency, during the relaxation delay between scans as well as during the mixing time in NOESY experiments, or by using a square-shaped pulse (100 ms for 0.6 s) defined by 1024 points.

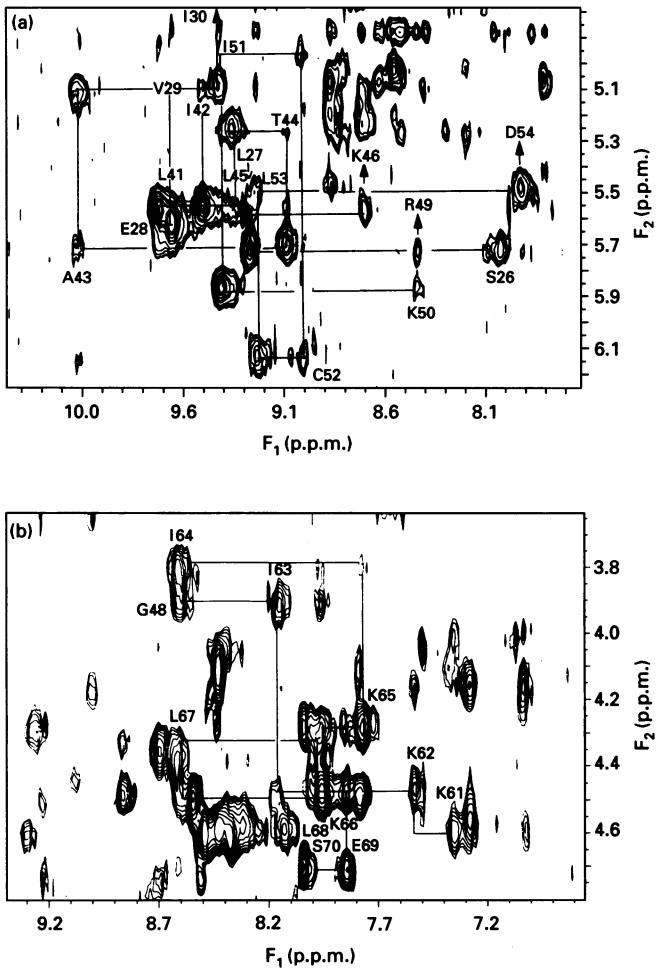

Figure 3 NOESY spectra of heparin-bound PF4-M2 αH-NH resonance region

The αH-NH resonance region from the NOESY contour plot shown in Figure 2(b), is given. Labelling of resonances is as discussed in the text. Some β-sheet (**a**) and C-terminal α-helix (**b**) sequences are connected by lines and TOCSY- or COSY-type cross-peak positions are indicated by residue labels.

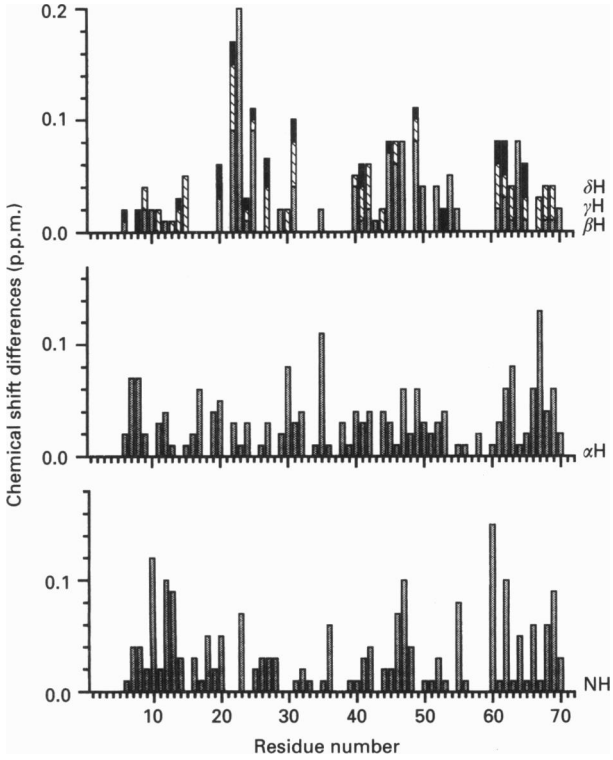

Figure 4 Chemical shift differences between PF4-M2 with and without heparin

The PF4-M2 protein sequence numbering is shown below with the absolute chemical shift difference between PF4-M2 in the absence and presence of heparin. NH, αH and $\beta/\gamma/\delta H_2$ shift differences are shown from bottom to top respectively.

The majority of 2D-NMR spectra were collected as 256 to 512 t_1 experiments, each with 1K complex data points over a spectral width of 6 kHz in both dimensions with the carrier placed on the water resonance. Either 64 or 96 scans were generally time-averaged per t_1 experiment. The data were processed offline on an X-32 based Bruker Aspect-1 workstation with the Bruker UXNMR and Aurelia programs. Data sets were multiplied in both dimensions by 30 to 60°-shifted sine-bell or Lorentzian to Gaussian transformation functions and generally zero-filled to 1K in the t_1 dimension prior to Fourier transformation.

RESULTS

PF4-M2 was titrated into a solution of heparin. The heterogeneous heparin molecular mass cut-off was 9000 Da (about 30 heparin saccharide residues per heparin molecule). The solution remained clear at heparin:PF4-M2 ratios above 2:1 to 2.5:1. At ratios less than 2:1, PF4-M2 formed a less soluble complex with heparin, resulting in precipitation at concentrations needed for the NMR work. The same observation was made with native PF4. This may indicate that two molecules of this lower-molecular-mass heparin bind to one molecule of PF4-M2. This is consistent with the work of Bock et al. [26] which indicates that PF4 can bind two molecules of lower-molecular-mass heparin and one molecule of high-molecular-mass heparin. To assure that the heparin–PF4 complex remained soluble during NMR studies, a ratio of 2.5:1 was used. The apparent K_d for the PF4-M2–heparin complex is 2×10^{-8} M [30], indicating that essentially all PF4-M2 is in the bound state.

NOESY spectra of PF4-M2 (32000 Da) in the presence and absence of heparin (9000 Da cut-off) are compared in Figures 2(a) and 2(b). Although cross-peaks for PF4-M2 are somewhat broader in the presence of heparin, chemical shift differences are minimal. If it is assumed that a 2:1 heparin–PF4-M2 complex is formed, most if not all of the apparent resonance broadening could be explained by the increased molecular mass of the complex, i.e. 50 kDa. In addition, some conformational heterogeneity induced by the binding of heterogeneous heparin to the protein could also contribute to apparent increases in linewidths.

Since resonance assignments for PF4-M2 already have been made in the absence of heparin [30], resonance assignments for PF4-M2 in the presence of heparin were made by spectral comparison and independently by using the standard sequential assignment approach [46] with HOHAHA and NOESY spectral analysis. The latter approach worked best for resonances belonging to β-sheet residues where HOHAHA (or COSY-type) cross-peaks were strongest. For resonances belonging to α-helix residues, HOHAHA cross-peaks were very weak. This clear

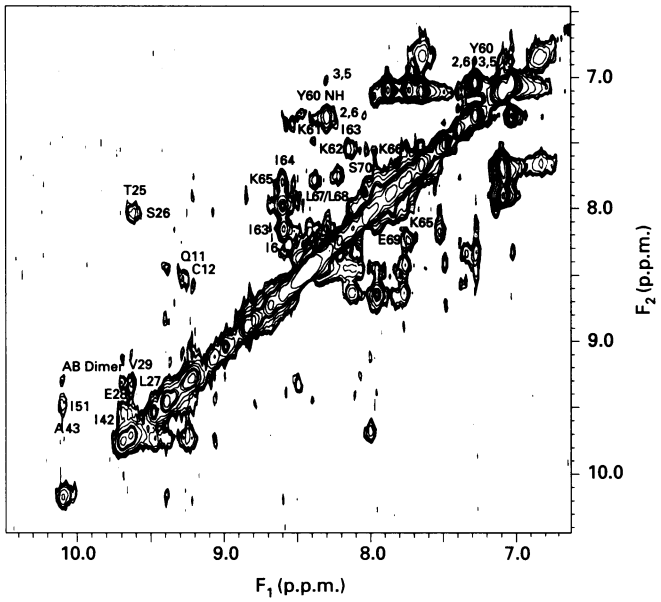

Figure 5 NOESY spectra of heparin-bound PF4-M2 NH-NH resonance region

The NH-NH resonance region from a NOESY contour plot is shown for heparin-bound PF4-M2. Conditions are as described in the legend to Figure 2. Labelling of resonances is as discussed in the text.

differentiability in HOHAHA cross-peak magnitudes is primarily the consequence of linewidths being considerably greater than $^3J_{\alpha N}$ coupling constants. Comparison of NOESY spectra in the presence and absence of heparin, therefore, provided more complete resonance assignment information. Variable mixing times also were used to distinguish intra- and inter-residue nuclear Overhauser effects (NOEs). When compared with free PF4-M2, backbone αH and NH assignments, in most cases, could readily be made. To exemplify the sequential assignments for heparin-bound PF4-M2, some β-sheet and C-terminal α-helix resonances have been traced out in NOESY spectra shown in Figures 3(a) and 3(b) respectively.

Initial inspection of chemical shift changes in the presence and absence of heparin indicates that heparin binding to PF4-M2 has no major conformational effect on the protein. The absolute values for chemical shift differences between free and heparin-bound PF4-M2 are shown in Figure 4. ^{1}H-resonance chemical shifts for free PF4-M2 were taken from Mayo et al. [30]. For backbone αH and NH resonances, average chemical shift differences are 0.03 p.p.m. and 0.04 p.p.m. respectively. Regions which are least affected are those containing β-sheet residues: Ser-26–Gly-33, Thr-38–Leu-45, and Lys-50–Leu-53. Residues in N-terminal, turn and C-terminal α-helix (Tyr-60–Ser-70) domains have their backbone resonances more perturbed on binding heparin. N-terminal and turn residues are more involved in AC and AD dimer quarternary structural interactions. Since these backbone resonances are among those shifted most, this may suggest some minor quarternary structural perturbations. Backbone resonance perturbations may be more the result of heparin dampening the internal mobility of the protein. PF4-M2 structural conservation in the presence of heparin is supported by NOE patterns and magnitudes exemplified in Figures 2 and 3. Figure 5 shows the NH-NH region from NOESY spectra of heparin-bound PF4-M2. As with free PF4-M2 [30], the C-terminal α-helix NH to NH NOEs, among others, are still present.

Several side-chain resonances are significantly shifted by the presence of heparin (Figure 3), indicating potential direct interactions with heparin. Arg-20, Arg-22, His-23, Thr-25, Leu-27, Lys-31, Leu-41, Ile-42, Leu-45, Lys-46, Asn-47, Arg-49, Lys-61, Lys-62 and Lys-65 side-chain resonances are most affected in this way. Leu-27, Leu-41, Ile-42 and Leu-45 are part of the hydrophobic core of PF4 [48,49] and may be shifted by indirect effects induced by heparin binding. Ile-64 is part of the C-terminal amphipathic helix and is sandwiched between the helix and the β-sheet core. For that matter, Ile-63, Leu-67 and Leu-68 are about equally shifted for similar reasons. All other shifted resonances belong to solvent-exposed hydrophilic residues, most of which are positively charged. C-terminal α-helix residues Lys-61, Lys-62, Lys-65 and Lys-66 are most often associated with PF4–heparin binding. Chemical shifts for Lys-66 side-chain resonances in the presence of heparin could not be determined, but presumably these too would be shifted. Arg-22, His-23, Thr-25, Lys-31 and Arg-49 resonances are more highly shifted than those of the C-terminal lysines, whereas the others, like Arg-20 and Lys-46, are about equally shifted. Although non-specific heparin binding could contribute to observed chemical shift changes, most major shift changes map to a ring of positive-charged residues on the surface of PF4-M2 (see below) as opposed to other charged residues. On the other hand, the possibility of multiple modes of interaction within this charged ring can not be excluded with the present data. This will be discussed further in the discussion section.

Figure 6 shows two views of the PF4-M2 tetramer. The view on the left is centred on the AD-dimer interface. C-terminal α-helices run antiparallel to each other at the top and bottom of this Figure. The van der Waals surfaces of potential heparin-binding residues discussed above are highlighted and labelled. Notice the spatial proximity of these positively charged residues. Although this positively charged band has been pointed out previously in a number of studies, this is the first experimental evidence that heparin interacts with numerous residues in this band. The view on the right-hand side (Figure 6) profiles the AD-dimer surface and shows that Arg-20 and Arg-22 are extended into the solvent where more effective contacts with heparin are possible. His-23, Lys-46 and Arg-49 lie in a broad crevice at the AD-dimer interface.

To probe the role of specific positively charged residues in heparin binding further, several site-directed mutants were made at Arg-20, Arg-22, Arg-49, Lys-61, Lys-62, Lys-65 and Lys-66. For the C-terminal α-helix domain, alanine was substituted for lysine as single, double and quadruple substitutions. This generated six mutants: K61A, K62A, K65A, K66A, K61,65A and K61,62,65,66A. Alanine was chosen to preserve high helix tendency [50]. Additionally, the KKIIKK sequence was replaced with QEIIQE to provide some opposite charge character to the positively charged band in PF4. In another mutant, Arg-20, Arg-22 and Arg-49 were simultaneously substituted with glutamines.

For all mutants, proper folding was assessed by CD and NMR data comparisons (results not shown) with PF4 and PF4-M2. From TOCSY and NOESY spectral comparisons, for example, the presence or absence of β-sheet and C-terminal α-helix folding could be readily determined by chemical shift dispersion and NOE patterns. Table 1 lists all mutant constructs and indicates whether or not they folded properly.

Interestingly, singly substituted C-terminal alanine mutants K61A and K65A were found to fold poorly on the basis of NOESY spectral comparisons, whereas doubly and quadruply substituted mutants K61,65A and K61,62,65,66A folded well.

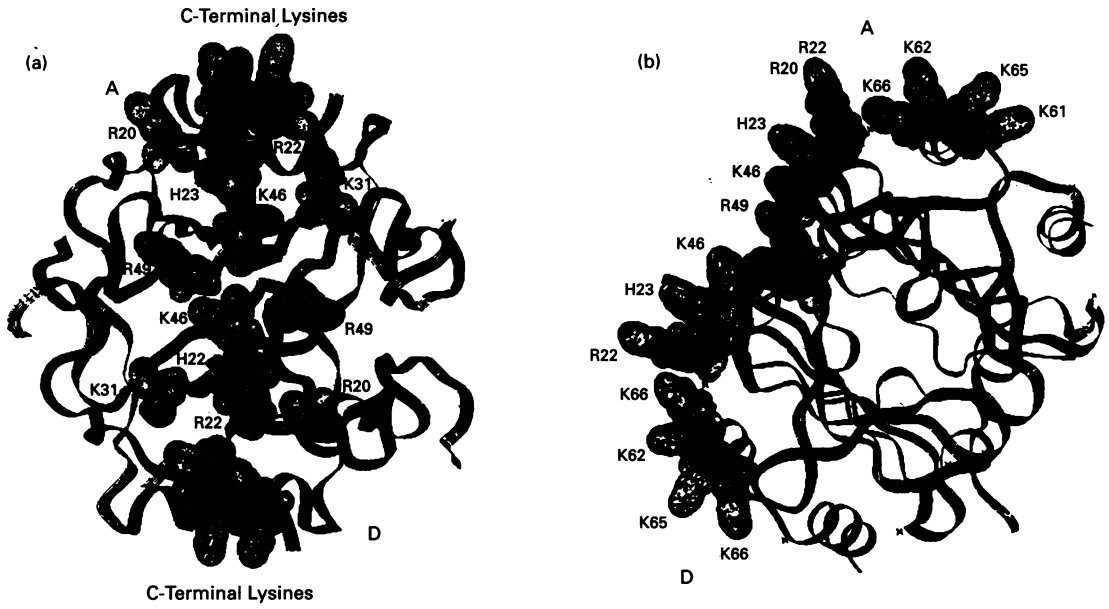

Figure 6 PF4-M2 AD-dimer interface

A view of the PF4-M2 AD-dimer interface (centred in the Figure) is shown in (**a**). The AD-dimer interface is profiled in (**b**). Data have been taken from Mayo et al. (unpublished work) for the NMR solution structure of PF4-M2. Some positively charged residues within the ring of positive charge that circumvents tetrameric PF4 are highlighted as discussed in the text.

Table 1 Folding and heparin-binding data for PF4 and some of its mutants

PF4 mutant	K_d (fluorescence)[a]	K_d (filter)[b]	K_d (salt)[c]	Folding[d]
Native PF4	2×10^{-8}	7×10^{-8}	18×10^{-8}	+
K61A	–	–	–	0
K62A	2×10^{-8}	8×10^{-8}	–	+
K65A	–	–	–	0
K66A	3×10^{-8}	8×10^{-8}	–	+
K61,65A	6×10^{-8}	10×10^{-8}	–	+
K61,62,65,66A	8×10^{-8}	11×10^{-8}	94×10^{-8}	+
QEIIQE[e]	1×10^{-5}	1×10^{-5}	–	+
Arg(R) → Gln(Q)[f]	14×10^{-8}	50×10^{-8}	1×10^{-5}	+

[a] Fluorescein-labelled heparin–PF4 fluorescence binding assay described in the Materials and methods section.
[b] [^{35}S]Heparin–PF4 filter binding assay described in the Materials and methods section.
[c] Heparin binding assayed in the presence of 0.5 M NaCl.
[d] Relative index of mutant PF4 folding judged by CD and NMR. '+' indicates native folding and '0' indicates either unfolded protein or poor folding.
[e] PF4 C-terminal sequence KKIIKK (61–66) substituted for QEIIQE.
[f] PF4 arginines Arg-20, Arg-22 and Arg-49 changed to Gln-20, Gln-22 and Gln-49.

While NOESY spectra for these singly substituted mutants K61A and K65A showed the absence of native folds, CD spectra showed the presence of secondary structure similar in composition to that of PF4. This could indicate the presence of 'molten globule'-like conformations, i.e. some secondary structure with a few fixed tertiary interactions [51]. Singly substituted mutants K62A and K66A and doubly substituted mutant K61,65A folded relatively well. These results indicate that the C-terminal lysines may play a role in PF4 protein folding. In PF4 and PF4-M2, Lys-61 and Lys-65 lie at the AB-dimer interface opposite Lys-65 and Lys-61, respectively, on the other subunit. If only one or the other of these lysines is present, proper AB-dimer folding may not occur. Lys-62 and Lys-66 lie on the opposite side of the helix, away from the AB-dimer interface.

Figure 7 and Table 1 shows heparin-binding data for those PF4 mutants which folded properly. Singly substituted mutants K62A and K66A showed minimal or no heparin-binding differences. Simultaneous substitution of two C-terminal lysines, i.e. PF4 K61,65A, showed a 3-fold decrease in heparin binding. Even with all four C-terminal lysines substituted for alanine, heparin binding to PF4 decreased by only a factor of four. However, when arginines were substituted, heparin binding fell off 7-fold. These relative changes in heparin binding also correlate with NMR chemical shift changes, which for arginines are greater than or equal to that for C-terminal lysines in the heparin-bound state. Three conclusions can be drawn: (1) PF4 can bind heparin even in the absence of some positively charged residues; (2) arginines are important for heparin binding; and (3)

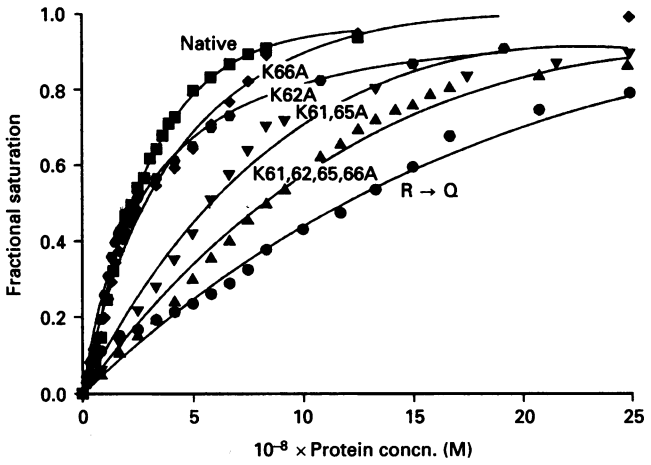

Figure 7 Heparin binding data for PF4 mutants

Heparin binding to PF4 and some PF4 mutants has been measured by the nitrocellulose filter and fluorescence binding assays described in the Materials and methods section. Binding curves are identified as follows: native PF4, solid square; PF4 mutant K62A, solid hexagon; PF4 mutant K66A, solid diamond; PF4 mutant K61,65A, solid triangles (down); PF4 mutant K61,62,65,66A, solid triangles (up); PF4 mutant R → Q, solid circle. These designations correspond to PF4 species listed in Table 1 and described in the text.

C-terminal lysines are less important to heparin binding than previously thought.

Addition of salt, i.e. NaCl, up to 0.5 M has a significant effect on the heparin binding of the arginine-substituted mutant, but less so on that of the lysine-substituted mutant PF4 K61,62,65,66A. For the lysine-substituted mutant, binding decreased about 8–9-fold, whereas for the arginine-substituted mutant, it decreased more than 20-fold. Considering that the net positive charge changed more with the lysine-substituted mutant (16 lysines/tetramer relative to 12 arginines/tetramer), this observation argues for a greater influence of arginines in modulating heparin binding.

Having said this, results with the C-terminal QEIIQE mutant, which is expressed and folds very well, were puzzling since at first glance these heparin-binding data could be used to argue for the importance of C-terminal lysines. However, in terms of the PF4-M2 structure [30] (and that of PF4 [52]), Glu-62 and Glu-66 would be proximal to Arg-20 and Arg-22 as shown in Figure 6 (Lys-62 and Lys-66). Direct electrostatic interactions, either attractive between these charged groups in PF4 (salt bridge formation) or repulsive between Glu-62/Glu-66 and heparin, could account for reduced heparin binding.

DISCUSSION

Heparin binding to PF4 apparently does not perturb the basic folding pattern in PF4-M2. Backbone resonances are, for the most part, only slightly chemically shifted. Compared with free PF4-M2 [30], NOEs that define the three-stranded antiparallel β-sheet domain and the C-terminal α-helix are still present at essentially the same magnitude. At this stage, quantitative comparisons of NOEs are not reliable since the heparin used is heterogeneous and may cause differential perturbations. The symmetry of PF4-M2 tetramer [30] may even be broken by heparin binding, albeit minimally since spectral perturbations are minor. Native bovine [28] and human [29] PF4s form asymmetric tetramers, while PF4-M2 [30] forms symmetric tetramers. Since PF4-M2 binds heparin almost as well as PF4 [30], tetramer asymmetry/symmetry is probably inconsequential to heparin binding. This aspect of the research will have to await the results of PF4–heparin-binding studies with homogeneous, well-defined heparin fractions currently underway.

Heparin and similar polysulphated glycosaminoglycan binding to proteins is modulated by electrostatic interactions. Positively charged residues Arg-20, Arg-22, His-23, Lys-31, Lys-46, Arg-49, Lys-61, Lys-62 and Lys-65 (and presummably Lys-66) are most perturbed on binding heparin. Thr-25 and Asn-47, both of which could donate and/or contribute hydrogen bonds to heparin, are two residues also apparently involved in PF4–heparin binding. PF4, like thrombin [53], generally has been thought of as binding heparin non-specifically due to the observation that the protein binds to glycosaminoglycans roughly in order of their negative charge density, that is, heparin $\geqslant$ heparan sulphate > dermatan sulphate > chondroitin sulphates > hyaluronic acid [27]. The question of non-specific PF4–heparin binding remains open. Some proteins are known to bind glycosaminoglycans in a differential and specific manner. For example, basic fibroblast growth factor-2 (FGF-2) interacts specifically with GlcN *N*-sulphate and IdoA 2-*O*-sulphate groups [54–56], while the GlcN 6-*O*-sulphates are redundant, neither contributing to nor interfering with FGF-2 binding [54–56]. In contrast, binding of hepatocyte growth factor to heparin/heparan sulphate appears to depend primarily on GlcN 6-*O*-sulphates [57]. While part of the PF4–heparin interaction may be of a non-specific nature, at least some of the binding may be promoted by specific interactions with arginine residues on PF4.

Analysis of the structures of bovine [28] and human [29,30] PF4 indicates that a ring of positive charge runs about the PF4 tetramer, orthogonal to the C-terminal α-helix axis. Stuckey et al. [32] have proposed that this ring forms the heparin-binding domain in PF4. This present study provides direct evidence that heparin does indeed interact with residues in this ring. As noted above, however, the four C-terminal α-helix lysines are not the most perturbed on binding heparin. For some time, chemical modification studies of PF4 positively charged groups [25] have been interpreted to indicate that these four C-terminal lysine residues form the PF4 heparin-binding domain. In fact, the present mutagenesis studies indicate that arginines are more effective than lysines at binding heparin. Both mutants, however, are still capable of binding heparin, albeit with weaker affinities. This supports the idea that several spatially related (as opposed to sequentially related) PF4 residues are necessary for heparin binding. Furthermore, increased ionic strength lowers the heparin affinity for the PF4 Arg → Gln mutant about 10–100-fold more than for the PF4 K61,62,65,66A mutant. This indicates that lysines may interact with heparin more non-specifically than do arginines.

Cardin and Weintraub [58] developed heparin-binding consensus sequences based heavily on the proposal that the PF4 C-terminal sequence containing the four lysines, i.e. LYKKIIKKLL, is the heparin-binding site. This present study indicates that their consensus binding sequences should be reviewed. Moreover, there is further compelling evidence from crystal structures of different heparin-binding proteins, such as (cleaved) antithrombin [59], lipoprotein lipase [60] and FGF-2 [61], that the key amino acids comprising heparin-binding domains are located in different peptide sequences that are spatially proximal. As a result of the tertiary structure of the protein, such sequences converge to form a composite glycosaminoglycan-binding site. This includes the ring of positive charge in PF4 noted above.

One of the key findings in this study is the observation that the arginine guanidino groups promote stronger PF4–heparin inter-

actions than the C-terminal lysine amine groups. This is consistent with observations made by others. By examining the frequency of amino acids in proteins in sites known to bind heparin as well as combinatorial peptides with high affinities for heparin and heparan sulphate agarose, Caldwell et al. (E. E. O. Caldwell, V. D. Nadkarni, J. R. Fromm, R. J. Lindhardt and J. M. Weiler, unpublished work) observed a preference for arginine over lysine, with histidine falling a distant third in modulating glycosaminoglycan binding. In the present study, His-23 C2 and C4 resonances showed significant chemical shifts in the presence of heparin. This is consistent with the observation of Talpas et al. [63], who indicated that the His-23 pK_a shifted significantly when bovine PF4 bound to heparin. This pK_a shift, however, may simply be a consequence of heparin binding to Arg-20 and Arg-22 that are proximal to His-23. Gelman et al. [64–66] demonstrated that polyarginine α-helix denatured at a higher temperature when binding to glycosaminoglycans than an analogous polylysine polymer [64]. GRG has been shown to preferentially interact with the uronic acid residue of heparin disaccharide and not to the more sulphated glucosamino residue (D. Mikhailov, K. H. Mayo, A. Pervin and R. J. Lindhardt, unpublished work), while GKG interacts non-selectively. From analysis of heparin-tripeptide equilibrium binding isotherms, Mascotti and Lohman [68] found that the tripeptides KWK and RWR bound heparin with association binding constants of $7.0 \times 10^3\ M^{-1}$ and $13 \times 10^3\ M^{-1}$ respectively. RWR bound heparin about 2-fold stronger than did KWK. Fromm et al. (J. R. Fromm, R. E. Hileman, E. E. O. Caldwell, J. M. Weiler and R. J. Linhardt, unpublished work) discovered that even blocked arginines bind more tightly to heparin than do blocked lysines, suggesting that hydrogen bonding of the arginine guanidino group to heparin plays a role in the binding process. Mascotti and Lohman [68] also concluded that arginines most likely participate in more extensive hydrogen bonding interactions with heparin. Arginines are also essential for the binding of thrombin and AT-III to heparin [70,71]. Arginines may have a structural feature in their basic side chain that enhances binding.

In structurally homologous phosphoryl–cation interactions, arginine also plays a more important role than does lysine or histidine. Conserved protein domains that bind phosphotyrosine (SH2 domains) contain more arginine than lysine residues [72,73] presumably due to the avid interaction of arginine with phosphoryl anions, compared with the interaction of lysine with the phosphoryl anion. From X-ray crystallographic and computer modelling studies ([74]; J. R. Fromm, R. E. Hileman, E. E. O. Caldwell, J. M. Weiler and R. J. Linhardt, unpublished work), it is apparent that guanidino groups can form fewer, albeit stronger, hydrogen bonds with sulphates/phosphates than do ammonium cations. The guanidino cation rather than the ammonium cation may form an inherently stronger electrostatic interaction with the sulphate anion. In the context of Pearson's concept of soft acid, soft base interactions [75], arginine, a large diffuse cation (soft), is ideally suited to interact with large (soft) bio-anions, such as sulphate and phosphate. Riordan and co-workers [76] suggest that in nature, arginyl residues play a unique role in anion recognition. It has even been suggested that arginine appeared later in evolution to perform important biological functions [76–78].

The PF4-M2 residues which are most chemically shifted by the binding to heparin lie within the ring of positive charge noted above. This is consistent with the PF4–heparin perpendicular (with respect to the C-terminal α-helix axis) binding model of Stuckey et al. [32] and refutes the original Cowan et al. [31] parallel binding model. The Stuckey et al. model [32], however, considers only a subset of possible orientations for heparin and the bovine PF4 complex and relies heavily on interactions with all four lysines. If this were so, one would expect to observe more significant chemical shift and PF4-mutant heparin binding changes for the C-terminal lysines.

Stuckey et al. [32] modelled the PF4–heparin interaction by centring the heparin chain on the C-terminal α-helix lysines, i.e. the C2 axis of symmetry of the AB dimer. The heparin molecule could bind to the helix bundle at some angle between the two limiting orientations, i.e. parallel or perpendicular, or could bind centrosymmetrically differently. An alternative mode of binding would have the heparin chain centred at the AD-dimer C2 symmetry axis. In this respect, the arginines and other important heparin-binding residues identified here would lie near the centre of this dimer and the C-terminal lysines would lie at the top and bottom of the AD-type dimer. This would better explain chemical shift perturbations and the fact that heparin binding is not highly perturbed by replacement of the C-terminal lysines. This possible novel orientation also agrees with the observations of Bock et al. [26] that PF4 binds two hexadecamers of heparin when the heparin fragments are in excess but only one molecule of larger heparins. A heparin molecule of 16 saccharide units still can bind one AD-type dimer without interfering with the other site; larger heparin molecules wrap around PF4 and occupy both sites. The inherent stability of the AB-type dimers [29,30] would help hold the tetrameric complex together. AC- and AD-type dimer interactions are considerably weaker than AB-type dimer interactions [19,28]. Resolution of this will have to await a high-resolution structure of the PF4–heparin complex. In particular, intermolecular protein–heparin NOEs need to be identified. In the present study, intermolecular proton–proton NOEs were not apparent for two possible reasons: (1) the presence of heterogeneous heparin and the possibility of multiple protein–heparin interactions; and (2) the dominance of electrostatic Coulombic binding forces, which may lead to large interproton distances between heparin and PF4-M2 and therefore to attenuated or absent intermolecular proton–proton NOEs.

Most of the basic residues identified here that interact with heparin are conserved in other members of the PF4 superfamily that are known to bind heparin [79], notably platelet basic protein, IL-8 and GRO-α. Stuckey et al. [32] have pointed out that the strength of the interaction generally correlates with the degree of conservation of the basic residues. Mayo [80] proposed that the aggregate state, i.e. monomer, dimer or tetramer, of the particular chemokine also contributes to the strength of glycosaminoglycan binding to the protein. This is one reason why tetrameric PF4 binds heparin more strongly than mostly monomeric platelet basic protein-related chemokines [33]. In the present study, the reduction of the net positive charge on tetrameric PF4 mutants affects heparin binding only slightly in some cases. If charge alone were responsible for the strength of heparin binding, then larger effects on PF4–heparin binding would have resulted.

Out of 11 CXC chemokines (sequences shown in Stuckey et al. [32] Figure 6), the loop 19–24 always begins and ends with a hydrophobic residue; residue 21 is always Pro (8/11) or Leu (3/11); positions 20, 22 and 23 are (with a single exception) always polar/charged with Arg or His in position 20, Arg or Lys in position 22, and His/Arg/Asn/Ser in position 23. The 45–49 loop is structurally conserved in bovine PF4 [28], human PF4 ([29]; K. H. Mayo, V. Roongta, E. Ilyina, R. Milius, S. Barker, C. Quinlan, G. La Rosa and T. J. Daly, unpublished work), IL-8 [81], Gro-α [82] and neutrophil-activating peptide-2 (NAP-2) [83]. Moreover, this sequence has been identified as a folding initiation site in PF4 [48,49]. With one exception out of the above-mentioned eleven, position 46 is Lys; position 48 is always

Gly; position 47 is usually Asn or Asp, and position 49 is mostly occupied by Arg (8/11). Lastly, the amphipathic C-terminal helix maintains a high incidence of lysines in all these species.

In summary, three conclusions can be drawn from this study: (1) PF4 can bind heparin even with the removal of some positively charged residues, (2) arginines are important for heparin binding, and (3) C-terminal lysines are less important to heparin binding than previously thought.

This work was supported by research support from the National Heart, Lung, and Blood Institute and Repligen Corporation to K.H.M., and by an American Heart Association, Minnesota Affiliate, Post-doctoral Fellowship to E.I.

REFERENCES

1 Deuel, T. F., Keim, P. S., Farmer, M. and Heinrikson, R. L. (1977) Proc. Natl. Acad. Sci. U.S.A. **74**, 2256–2258
2 Wolpe, S. D. and Cerami, A. (1989) FASEB J. **3**, 2565–2573
3 Davie, E. W., Fujikawa, K. and Kisiel, W. (1991) Biochemistry **30**, 10363–10370
4 Laterra, J., Silbert, J. E. and Culp, L. A. (1983) J. Cell Biol. **96**, 112–123
5 Brindley, L. L., Sweet, J. M. and Goetzl, E. J. (1983) Clin. Invest. **72**, 1218–1223
6 Deuel, T. F., Senior, R. M., Chuang, D., Griffin, G. L. and Heinrikson, R. L. (1981) Proc. Natl. Acad. Sci. U.S.A. **78**, 4584–4587
7 Osterman, G. D., Griffin, G. L., Senior, R. M., Kaiser, E. T. and Deuel, T. F. (1982) Biochem. Biophys. Res. Commun. **107**, 130–135
8 Senior, R. M., Griffin, G. L., Huang, J. S., Walz, D. A. and Deuel, T. F. (1983) J. Cell Biol. **96**, 382–385
9 Capitanio, A. M., Niewiarowski, S., Rucinski, B., Tuszynski, G. P., Cierniewski, C. S., Hershock, D. and Kornecki, E. (1985) Biochim. Biophys. Acta **839**, 161–173
10 Lonky, S. A. and Wohl, H. (1981) J. Clin. Invest. **67**, 817–826
11 Bebawy, S. T., Gorka, J., Myers, T. M. and Webster, R. O. (1986) J. Leuk. Biol. **39**, 423–434
12 Zucker, M. B., Katz, I. R. and Thorbecke, G. J. (1985) Blood **66**, 1148 (abstract)
13 Gerwitz, A. M., Calabretta, B., Rucinski, B., Niewiarowski, S. and Xu, W. Y. (1989) J. Clin. Invest. **83**, 1477–1486
14 Han, Z. C., Sensebe, L., Abgrall, J. F. and Briere, J. (1990) Blood **75**, 1234–1239
15 Maione, T. E., Gray, G. S., Petro, J., Hunt, A. J., Donner, A. L., Bauer, S. I., Carson, H. F. and Sharpe, R. J. (1990) Science **247**, 77–79
16 Sharpe, R. J., Byers, H. R., Scott, C. F., Bauer, S. I. and Maione, T. E. (1990) J. Natl. Cancer Inst. **82**, 848–853
17 Sato, Y., Abe, M. and Takaki, R. (1990) Biochem. Biophys. Res. Commun. **172**, 595–600
18 Holt, J. C. and Niewiarowski, S. (1985) Semin. Hematol. **22**, 151–163
19 Mayo, K. H. and Chen, M. J. (1989) Biochemistry **28**, 9469–9478
20 Huang, S. S., Huang, J. S. and Deuel, T. (1982) J. Biol. Chem. **257**, 11546–11550
21 Barber, A. J., Kaser-Blanzmann, R., Jakabova, M. and Luscher, E. F. (1972) Biochim. Biophys. Acta **286**, 312–328
22 Perlin, A. S., Mackie, D. M. and Dietrich, C. P. (1971) Carbohydr. Res. **18**, 185–192
23 Lindahl, U. (1974) Int. Rev. Sci., Org. Chem. Ser. 2 **7**, 283–289
24 Jeanloz, R. W. (1975) Adv. Exp. Med. Biol. **52**, 3–12
25 Loscalzo, J., Melnick, B. and Handin, R. I. (1985) Arch. Biochem. Biophys. **24**, 446–455
26 Bock, P. E., Luscombe, M., Marshall, S. E., Pepper, D. S. and Holbrook, J. J. (1980) Biochem. J. **191**, 769–776
27 Handin, R. I. and Cohen, H. J. (1976) J. Biol. Chem. **251**, 4273–4282
28 St. Charles, R., Walz, D. A. and Edwards, B. F. P. (1989) J. Biol. Chem. **264**, 2092–2099
29 Zhang, X., Chen, L. and Bancroft, D. P. (1994) Biochemistry **33**, 8361–8366
30 Mayo, K. H., Roongta, V., Ilyina, E., Milius, R., Barker S., Quinlan, C., La Rosa, G. and Daly, T. J. (1995) Biochemistry **34**, 11399–11409
31 Cowan, S., Bakshi, E. N., Machin, K. J. and Issacs, N. W. (1986) Biochem. J. **234**, 485–488
32 Stuckey, J. A., St. Charles, R. and Edwards, B. F. P. (1992) Proteins: Struct. Func. Genet. **14**, 277–287
33 Yang, Y., Mayo, K. H., Daly, T. J., Barry, J. K. and La Rosa, G. L. (1994) J. Biol. Chem. **269**, 20110–20118
34 Suda, Y., Sobel, M., Sumi, M. and Ottenbride, R. M. (1990) J. Bioact. Compatible Polymers **5**, 412–419
35 Smith, P. K., Krohn, R. I., Hermanson, G. T., Mallia, A. K., Gartner, F. H., Provenzano, M. D., Fujimoto, E. K., Goeke, N. M., Olson, B. J. and Klenk, D. C. (1985) Anal. Biochem. **150**, 76–85
36 Bidlingmeyer, B. A., Cohen, S. A. and Tarvin, T. L. (1984) J. Chromatogr. **336**, 93–100
37 Lowry, O. H., Rosbough, N. J., Fan, A. L. and Randall, R. J. (1951) J. Biol. Chem. **193**, 265–270
38 Waddell, W. J. (1956) J. Lab. Clin. Med. **48**, 311–314
39 Aue, W. P., Bartholdi, E. and Ernst, R. R. (1976) J. Chem. Phys. **64**, 2229–2246
40 Wider, G., Macura, S., Anil-Kumar, Ernst, R. R. and Wuthrich, K. (1984) J. Magn. Reson. **56**, 207–234
41 Piantini, U., Srensen, O. W. and Ernst, R. R. (1982) J. Am. Chem. Soc. **104**, 6800–6805
42 Shaka, A. J. and Freeman, R. (1983) J. Magn. Reson. **51**, 161–169
43 Reference deleted.
44 Jeener, J., Meier, B., Backman, P. and Ernst, R. R. (1979) J. Chem. Phys. **71**, 4546–4550
45 Bax, A. and Davis, D. G. (1985) J. Magn. Reson. **65**, 355–360
46 Wüthrich, K. (1986) NMR of Proteins and Nucleic Acids, Wiley-Interscience, NY
47 States, D. J., Haberkorn, R. A. and Ruben, D. J. (1982) J. Magn. Reson. **48**, 286–293
48 Ilyina, E., Milius, R. and Mayo, K. H. (1994) Biochemistry **33**, 13436–13444
49 Ilyina, E. and Mayo, K. H. (1995) Biochem. J. **306**, 407–419
50 Chou, P. Y. and Fasman, G. D. (1978) Adv. Enzymol. Relat. Areas Mol. Biol. **48**, 45–148
51 Jaenicke, R. (1991) Biochemistry **30**, 3147–3161
52 Zhang, X., Chen, L. and Bancroft, D. P. (1994) Biochemistry **33**, 8361–8366
53 Olson, S. T., Halvorson, H. R. and Bjork, I. (1991) J. Biol. Chem. **266**, 6342–6352
54 Maccarana, M., Casu, B. and Lindahl, U. (1993) J. Biol. Chem. **268**, 23898–23905
55 Habuchi, H., Suzuki, S., Saito, T., Tamura, T., Harada, T., Yoshida, K. and Kimata, K. (1992) Biochem. J. **285**, 805–813
56 Turnbull, J. E., Fernig, D. G., Ke, Y., Wilkinson, M. C. and Gallagher, J. T. (1992) J. Biol. Chem. **267**, 10337–10341
57 Lyon, M., Deakin, J. A., Mizuno, K., Nakamura, T. and Gallagher, J. T. (1994) J. Biol. Chem. **269**, 11216–11223
58 Cardin, A. D. and Weintraub, H. J. R. (1989) Arteriosclerosis **9**, 21–32
59 Mourey, L., Samama, J. P., Delarue, M., Pepitou, M., Choay, J. and Moras, D. (1993) J. Mol. Biol. **232**, 223–241
60 van Tilbeurgh, H., Roussel, A., Lalouel, J. M. and Cambillau, C. (1994) J. Biol. Chem. **269**, 4626–4633
61 Eriksson, A. E., Cousens, L. S. and Matthews, B. W. (1993) Protein Sci. **2**, 1274–1284
62 Reference deleted.
63 Talpas, C. J., Walz, D. A. and Lee, L. (1991) Biochim. Biophys. Acta **1078**, 208–218
64 Gelman, R. A. and Blackwell, J. (1974) Biopolymers **13**, 139–156
65 Gelman, R. A., Glasnr, D. N. and Blackwell, J. (1973) Biopolymers **12**, 1223–1232
66 Gelman, R. A., Rippon, W. B. and Blackwell, J. (1973) Biopolymers **12**, 541–558
67 Reference deleted.
68 Mascotti, D. P. and Lohman, T. M. (1995) Biochemistry **34**, 2908–2915
69 Reference deleted.
70 Pomerantz, M. W. and Owen, W. G. (1978) Biochim. Biophys. Acta **535**, 66–77
71 Machovich, R., Staub, M. and Patthy, L. (1978) Eur. J. Biochem. **83**, 473–477
72 Koch, C. A., Anderson, D., Moran, M. F., Ellis, C. and Pawson, T. (1991) Science **252**, 668–674
73 Waksman, G., Shoelson, S. E., Pant, N., Cowburn, D. and Kuriyan, J. (1993) Cell **72**, 779–790
74 Cotton, F. A., Hazen, E. E., Day, V. W., Larsen, S., Norman, J. G., Wong, S. T. K. and Johnson, K. H. (1973) J. Am. Chem. Soc. **95**, 2367–2369
75 Pearson, R. G. (1963) J. Am. Chem. Soc. **85**, 3533–3539
76 Riordan, J. F., McElvany, K. D. and Borders, C. L., Jr. (1977) Science **195**, 884–886
77 Wallis, M. (1974) Biochem. Biophys. Res. Commun. **56**, 711–716
78 Jukes, T. H. (1973) Biochem. Biophys. Res. Commun. **53**, 709–714
79 Witt, D. P. and Lander, A. D. (1994) Curr. Biol. **4**, 394–400
80 Mayo, K. H. (1991) Biochemistry **30**, 925–934
81 Clore, G. M., Appella, E., Yamada, M., Matsushima, K. and Gronenborn, A. M. (1989) Biochemistry **29**, 1689–1696
82 Fairbrother, W. J., Reilly, D., Colby, T. J., Hesselgesser, J. and Horak, R. (1994) J. Mol. Biol. **242**, 252–270
83 Mayo, K. H., Yang, Y., Daly, T. J., Barry, J. K. and La Rosa, G. J. (1994) Biochem. J. **304**, 371–376

Received 24 May 1995/13 July 1995; accepted 24 July 1995